Exploring the arsenic removal potential of various biosorbents from water

Muhammad Bilal Shakoor[a,b], Nabeel Khan Niazi[a,c,*], Irshad Bibi[a,*], Muhammad Shahid[d], Zulfiqar Ahmad Saqib[a], Muhammad Farrakh Nawaz[e], Sabry M. Shaheen[f,g], Hailong Wang[h,i], Daniel C.W. Tsang[j], Jochen Bundschuh[k], Yong Sik Ok[l], Jörg Rinklebe[g,m]

[a] Institute of Soil and Environmental Sciences, University of Agriculture Faisalabad, Faisalabad 38040, Pakistan
[b] Department of Environmental Sciences and Engineering, Government College University Faisalabad, Faisalabad 38000, Pakistan
[c] School of Civil Engineering and Surveying, University of Southern Queensland, Toowoomba 4350, Queensland, Australia
[d] Department of Environmental Sciences, COMSATS University Islamabad, Vehari Campus. Vehari- 61100, Pakistan
[e] Department of Forestry and Range Management, University of Agriculture Faisalabad, Faisalabad 38040, Pakistan
[f] Department of Soil and Water Sciences, Faculty of Agriculture, University of Kafrelsheikh, 33516 Kafr El-Sheikh, Egypt
[g] Laboratory of Soil- and Groundwater-Management, Institute of Foundation Engineering, Water- and Waste-Management, School of Architecture and Civil Engineering, University of Wuppertal, Pauluskirchstraße 7, 42285 Wuppertal, Germany
[h] Key Laboratory of Soil Contamination Bioremediation of Zhejiang Province, Zhejiang A & F University, Lin'an, Hangzhou 311300, China
[i] School of Environment and Chemical Engineering, Foshan University, Foshan 528000, China
[j] Department of Civil and Environmental Engineering, The Hong Kong Polytechnic University, Hung Hom, Kowloon, Hong Kong, China
[k] UNESCO Chair on Groundwater Arsenic within the 2030 Agenda for Sustainable Development, University of Southern Queensland, West Street, Toowoomba, 4350, Queensland, Australia
[l] O-Jeong Eco-Resilience Institute (OJERI), Division of Environmental Science and Ecological Engineering, Korea University, Seoul 02841, Republic of Korea
[m] Department of Environment, Energy and Geoinformatics, Sejong University, 98 Gunja-Dong, Guangjin-Gu, Seoul, South Korea

ARTICLE INFO

ABSTRACT

Globally, contamination of groundwater with toxic arsenic (As) is an environmental and public health issue given to its carcinogenic properties, thereby threatening millions of people relying on drinking As-contaminated well water. Here, we explored the efficiency of various biosorbents (egg shell, java plum seed, water chestnut shell, corn cob, tea waste and pomegranate peel) for arsenate (As(V)) and arsenite (As(III)) removal from As-contaminated water. Significantly, egg shell and java plum seed displayed the greatest As(III) elimination (78–87%) at 7 pH followed by water chestnut shell (75%), corn cob (67%), tea waste (74%) and pomegranate peel (65%). In contrast, 71% and 67% of As(V) was removed at pH 4.1 and 5.3 by egg shell and java plum seed, respectively. The maximum As(V) and As(III) sorption by all the biosorbents was obtained, notably for egg shell and java plum seed, after 2 h contact time. Langmuir isotherm and pseudo-second order models best fitted the sorption data for both forms of As. The –OH, –COOH, –NH$_2$ and sulfur-bearing surface functional groups were possibly involved for As(III) and As(V) removal by biosorbents. The scanning electron microscopy combined with the energy dispersive X-ray spectroscopy (SEM-EDX) analysis showed that the heterogeneous surface of biosorbents, possessing rough and irregular areas, could have led to As sorption. Both As(V) and As(III) were successfully desorbed (up to 97%) from the biosorbents in four sorption/desorption (regeneration) cycles. This pilot-scale study highlights that egg shell and java plum seed have the greatest ability to remove both As species from As-contaminated drinking water. Importantly, these findings provide insights to develop an inexpensive, effective and sustainable filtration technology for the treatment of As in drinking water, particularly in developing countries like Pakistan.

1. Introduction

Arsenic (As) is a naturally occurring metalloid and abundantly found in the Earth's crust (Singh et al., 2015; Khalid et al., 2017). Natural processes including weathering of As-rich minerals and anthropogenic sources such as poorly managed discharge from metallurgical and mining industries, and application of As-containing pesticides are major sources of As in groundwater (Shahid et al., 2017; Niazi et al., 2018a). Inorganic As species, such as arsenate (As(V)) and arsenite (As(III)) are major contributors in groundwater As

contamination (Naidu et al., 2006; Shakoor et al., 2015). Arsenate is stable and predominates under oxidizing environments (e.g., surface water/shallow groundwater), while As(III) prevails in reducing conditions (Smedley and Kinniburgh, 2002; Zhang et al., 2016). Arsenite is considered to be 60 times more mobile and toxic compared to As(V) (Meharg and Rahman, 2003; Niazi et al., 2017).

Geogenically released As to groundwater has emerged as a health and environmental issue throughout the world. In many countries, groundwater pumped from millions of wells is highly contaminated with As (up to $3500\,\mu g\,L^{-1}$) which are the sole source of drinking water for people in many of the developing countries worldwide (Rasheed et al., 2016; Waqas et al., 2017). Intake of As-contaminated drinking water from wells has become a serious public health risk which has impacted > 200 million people globally (Smedley and Kinniburgh, 2002). Groundwater of many countries such as Australia, the USA, Mexico, Argentina, Canada, Chile, Poland, Taiwan, Japan, Hungry, Vietnam, China, Nepal, Iran, India, Bangladesh and Pakistan has been affected with As poisoning (Smedley and Kinniburgh, 2002; Singh et al., 2015).

Given the toxic and carcinogenic effects of As (Hsu et al., 2016; Shakoor et al., 2017), World health Organization (WHO) has recommended $10\,\mu g\,L^{-1}$ as safe limit of As in drinking water (Shakoor et al., 2015). In the last two decades, several remedial methods have been developed to eliminate toxic As from water. However, for maintaining As concentration within the WHO permissible limit in potable water, scientific community is seeking innovative and low-cost solutions for water treatment and updating the current treatment technologies.

Previous research, although partly, has focused to develop efficient and cost-effective sorbents for treatment of As-contaminated water such as nano-particles of iron oxides, ion exchange resins, activated carbon and gels (Abid et al., 2016; Dadwal and Mishra, 2016). The concept of using cheap and easily available materials has grown quickly, which involved the utilization of solid biowastes (known as 'biosorbents') – the byproducts from food-industry and agricultural wastes (Shaheen et al., 2015; Ashraf et al., 2017). The potential benefits of biosorption over the conventional other techniques include easy/local availability, low operating cost, less energy requirements, minimum sludge production, reuse of biosorbent, high removal efficiency and possibility of element recovery (Tajernia et al., 2014; Niazi and Burton, 2016; Shakoor et al., 2016).

The biochemical composition of these biosorbents comprise of lignin, cellulose, hemicellulose, simple sugars, proteins, lipids, starch and water hydrocarbons containing different kinds of surface functional groups (i.e., hydroxyl, carboxyl and amide) – which can facilitate complexation and help in removing As and/or other potentially toxic elements from contaminated water (Kaartinen et al., 2017; Mondal and Garg, 2017). In the last decade, agriculture and food-industry biowastes including sugarcane bagasse, orange peel, water melon rind, coconut shell, and rice husk have been used as potential biosorbents to immobilize As from water (Bibi et al., 2017; Hering et al., 2017; Shakoor et al., 2018).

However, research is required for exploring the new biosorbents, as well as mechanisms of their interactions with As and highlight underlying mechanisms of As(V) and As(III) biosorption on the surface under a range of environmentally-relevant aqueous environments. Here, we explored and compared the efficiency of various previously unexplored biosorbents (corn cob, water chestnut shell, java plum seed, tea waste, egg shell and pomegranate peel) for As(III) and As(V) elimination from water along with their reusability potential through sorption/desorption cycles. The specific aims of this study were achieved by appraising the varying pH (pH 3 to 10), biosorbent dose, initial As(III) and As(V) concentrations, contact time and assessing the As desorption (reusability) up to four sorption/desorption cycles. The macroscopic sorption data were complemented with integrated microscopic and spectroscopic techniques, and sorption isotherm and kinetic modeling

for delineating As removal potential and possible mechanisms by the biosorbents.

2. Materials and methods

2.1. Materials

Stock solutions were prepared using Milli Q water (resistivity, 18.2 MΩ cm; Millipore Corp.), and all the chemicals and reagents used were of analytical grade. Arsenate and As(III) stock solutions of $1000\,mg\,L^{-1}$ concentration were prepared by using required amounts of disodium hydrogen arsenate ($Na_2HAsO_4.7H_2O$) and sodium arsenite ($NaAsO_2$), respectively. The glassware and plastic used in batch sorption experiments were completely washed in 2% HNO_3 followed by two times washing with deionized water (DW).

2.2. Preparation of biosorbents

Six types of biowastes used (corn cob, water chestnut shell, java plum seed, tea waste, egg shell and pomegranate peel) were obtained from a local market in Faisalabad (Pakistan). The collected biowaste materials were washed carefully with DW to eradicate dirt followed by sun-drying for two days and oven drying for 3 days at 65 °C. The materials (hereafter referred to as biosorbents) were ground and sieved (< 250 μm) to obtain a consistent size.

2.3. Experimentation

Sorption laboratory experiments were carried out in a batch system using plastic vials (50 mL) and background electrolyte solution of NaCl (0.01 M) was employed in all the experiments. All the experiments were carried out in triplicate at 20 ± 1 °C for 2 h equilibration time.

In the isotherm study, initial As(III) or As(V) concentration spanned 0.01 to $7\,mg\,L^{-1}$, keeping in view the varying As concentration observed in a range of aquatic environments as described elsewhere (Niazi et al., 2018a).

The effect of pH (pH 3–10), biosorbent dose ($1–16\,g\,L^{-1}$) and contact time were investigated at an initial As(III) or As(V) concentration of $4\,mg\,L^{-1}$ for pH and contact time studies, and $5\,mg\,L^{-1}$ for biosorbent dose study.

Kinetic experiments were used to evaluate the influence of contact time (0.016–24 h) on As(V) and As(III) sorption at a constant pH (optimized from the sorption edge (pH) experiments).

For the kinetic and isotherm experiments, pH was selected from the sorption edge experiment whereby biosorbents achieved the maximum As sorption in As-containing aqueous solution ($4\,mg\,L^{-1}$). For As(III) biosorption, pH was set at 7.0 for the water chestnut shell, java plum seed, corn cob, tea waste, egg shell, and at pH 9 for pomegranate peel. For As(V) experiments, pH was maintained at 4.1 for the water chestnut shell, tea waste, egg shell, pomegranate peel, 5.3 for java plum seed and 6.0 for corn cob (based on their maximum As(III) or As(V) sorption obtained from sorption edge experiments)).

A constant (optimized) biosorbent dose ($1\,g\,L^{-1}$) was employed for all the sorption experiments. After achieving equilibrium (2 h), centrifugation (4000 rpm) was done and the suspensions were filtered (0.45 μm) and preserved (4 °C) for As analysis using a hydride generation atomic absorption spectrometer (HG-AAS) (Agilent, model No. 200 series AA as described by Niazi et al. (2018b)). Triplicate samples were used for the experiments and data for As analysis are displayed as mean ± standard error.

The As removal (%) from water was computed as given below (Eq. (1)):

$$\%As\ removal = \frac{C_o - C_e}{C_o} \times 100 \tag{1}$$

where C_o is the initial concentration ($mg\,L^{-1}$) of As in solution and C_e

shows the equilibrium As concentration (mg L^{-1}). The sorption capacity (q_e) (mg g^{-1}) was obtained (Eq. (2)):

$$q_e = \frac{(C_o - C_e)\, V}{m} \qquad (2)$$

where, m is biosorbent dry mass (g) and V is volume (L) of aqueous solution.

2.4. Sorption/desorption (regeneration) experiments

Sorption/desorption batch experiments were done to examine the reusability of biosorbents used in this study. At first, HCl and NaOH (0.1 and 0.5 M) solutions were applied for desorption of As(V) and As(III) (data not shown), and interestingly 0.1 M NaOH solution was successful in desorption of both As species compared to other solutions. Therefore, desorption was done using 25 mL of 0.1 M NaOH solution in four cycles (each for 40 min) – considering the maximum As desorption upto the fourth cycle. Arsenic contents in the sample obtained after completion of every cycle was analyzed as described above. The percent As desorption was computed by Eq. (3).

$$\%As\ desorption = \frac{C_{o\ des}}{C_{sorb}} \times 100 \qquad (3)$$

where, C_{des} (mg L^{-1}) and C_{sorb} (mg L^{-1}) are As released in the solution and sorbed onto biosorbent.

2.5. Modeling for As sorption

Sorption isotherm and kinetic models were employed to describe As (V/III) sorption by six biosorbents tested here (Prasad et al., 2014; Niazi et al., 2018a). The details of modeling can be found in Supplementary material (Appendix A). For isotherm and kinetic modeling Microsoft® Excel 2010 and Sigma Plot version 10 were used.

2.6. Functional groups characterization and SEM-EDX analyses

Fourier transform infrared (FTIR) spectroscopy (Model Excalibur 3000MX; Bio-Rad, Hercules, USA) was used for the characterization of surface functional groups of biosorbents. Absorbance spectra were obtained in the wavenumber ranging from 400 to 4000 cm^{-1} with 32 consecutive scans at the resolution of 4 cm^{-1} following the potassium bromide pellet method as described elsewhere (Igalavithana et al., 2017). The FTIR absorbance spectra were baseline corrected and normalized by using the Essential FTIR software (version 2.00.045); the representative peaks of the surface functional groups were identified using the literature.

The morphology (surface) and elemental composition of the biosorbents were determined using scanning electron microscopy combined with the energy dispersive X-ray spectroscopy (SEM-EDX; Model SU8000, Hitachi, Japan) as reported in our earlier study (Igalavithana et al., 2017).

Specific surface area (SSA) of all six biosorbents was determined by the method of Brunauer-Emmett-Teller (BET) (Walton and Snurr, 2007). The SSA of the biosorbents used in the current study ranged from 3.96 to 7.91 m^2 g^{-1} (Table 1). The egg shell (7.91 m^2 g^{-1}) and

Table 1
Specific surface area of the six biosorbents.

Biosorbents	Specific surface area (m^2 g^{-1}) (n = 3)
Egg shell	7.91 ± 0.49
Java plum seed	6.99 ± 0.61
Water chestnut shell	6.91 ± 0.42
Corn cob	4.16 ± 0.57
Tea waste	4.03 ± 0.61
Pomegranate peel	3.96 ± 0.72

java plum seed (6.99 m^2 g^{-1}) showed the highest SSA.

3. Results and discussion

3.1. Influence of pH

3.1.1. Arsenite sorption

The pH is an important factor which affects the overall performance of biosorption process through direct influence aqueous behavior of sorbate (As) and surface properties of the sorbent (Ghimire et al., 2003; Marín-Rangel et al., 2012; Narayanan and Dhamodaran, 2014). Results of Figs. 1a–f and 2a–f demonstrated that sorption potential of all the biosorbents for As(III) was pH dependent, thus showing a maximum removal of As(III) at pH 7.0 with initial As(III) concentration of 4–5 mg L^{-1}. While additional increase in the pH (> 7.5) decreased As biosorption for all the biosorbents tested in this study, except for the pomegranate peel (Figs. 1 and 2). These results are in good agreement with those acquired for mango leaf powder and burnt rice straw, whereby maximum As(III) was depleted at pH 7 indicating a decrease in As(III) sorption with increasing pH (Faruque and Uddin, 2012; Kamsonlian et al., 2012).

Among the six biosorbents, egg shell showed the maximum As(III) removal (85%) followed by java plum seed (78%), water chestnut shell (75%), corn cob (67%), tea waste (74%) and pomegranate peel (65%) (Fig. 2a, b). In the pH range of 7–9, dominant monoanionic (H$_2$AsO$_3^-$) and neutral (H$_3$AsO$_3$) As(III) species could be sorbed by replacing hydroxyl (–OH) ions or water molecules on the biosorbents. Neutral As species (H$_3$AsO$_3$) cannot interact electrostatically with the biosorbent in this pH range. However, H$_2$AsO$^-$ can bind with amino (–NH$_2$) groups (unprotonated) of biosorbents and remove As(III) from water (Aryal et al., 2010; Niazi et al., 2018b). The decrease in As(III) biosorption at high pH > 7.5 could be attributed to the competition between –OH ions and anionic As(III) forms for sorption sites (Prasad et al., 2014; Mehmood et al., 2017).

Biosorbents possess surface functional groups including –OH, carboxyl (–COOH) and –NH$_2$ on their surface which can become negatively charged at alkaline conditions (pH > 7.0) producing overall negative charge on the surface of biosorbent (Abid et al., 2016). The possession of net negative charge on biosorbent at elevated pH could form a repulsive environment between anionic species of As(III) (H$_2$AsO$_3^-$ having pKa value of 9.22) (which remain in water) and negatively charged biosorbent thus leading to decreased sorption of biosorbent with increasing at pH (8–10) (Sari and Tuzen, 2009; Niazi et al., 2015).

3.1.2. Arsenate sorption

It was noted that As(V) sorption increased with rising pH from 3 to 6.5 having a maximum removal of 71% by egg shell at pH 4 and 69% by java plum seed at pH 5.3 (Fig. 5a, b). A significant decline in As(V) sorption was observed with the increasing pH for all biosorbents. Similar trend was also found for As(V) sorption on orange peel and wheat straw by Abid et al., (2016) and Ebrahimi et al., (2014), respectively. In our study, highest As(V) sorption was found at pH 4–6.5 (Figs. 1 and 2) because at this pH range common As(V) species in water are H$_2$AsO$_4^-$ and HAsO$_4^{2-}$ ions, which could make strong bonds on biosorbents by replacing –OH/–COOH ligands (Ebrahimi et al., 2014; Niazi et al., 2012).

For the pH 4–10, aqueous As(V) speciation is largely controlled by H$_2$AsO$_4^- \leftrightarrow$ HAsO$_4^{2-}$ + H$^+$ at 7.01 pKa value (Sari and Tuzen, 2009; Niazi et al., 2011). The surface charge of biosorbents can be positive at pH below 7.0 and transformed to negative above 7.0 (Prasad et al., 2014). Hence, a decline in sorption at pH above 7.0 could be due to electrostatic repulsive reactions between similarly charged (negative), –OH/–COOH, groups of the biosorbents and aqueous As(V) (Prasad et al., 2014). Moreover, at the pH > 7.0, negative ions such as –OH prevail in water and thus sorption could be unfavorable owing to the competition between aqueous As(V) and –OH ions for sorption sites on
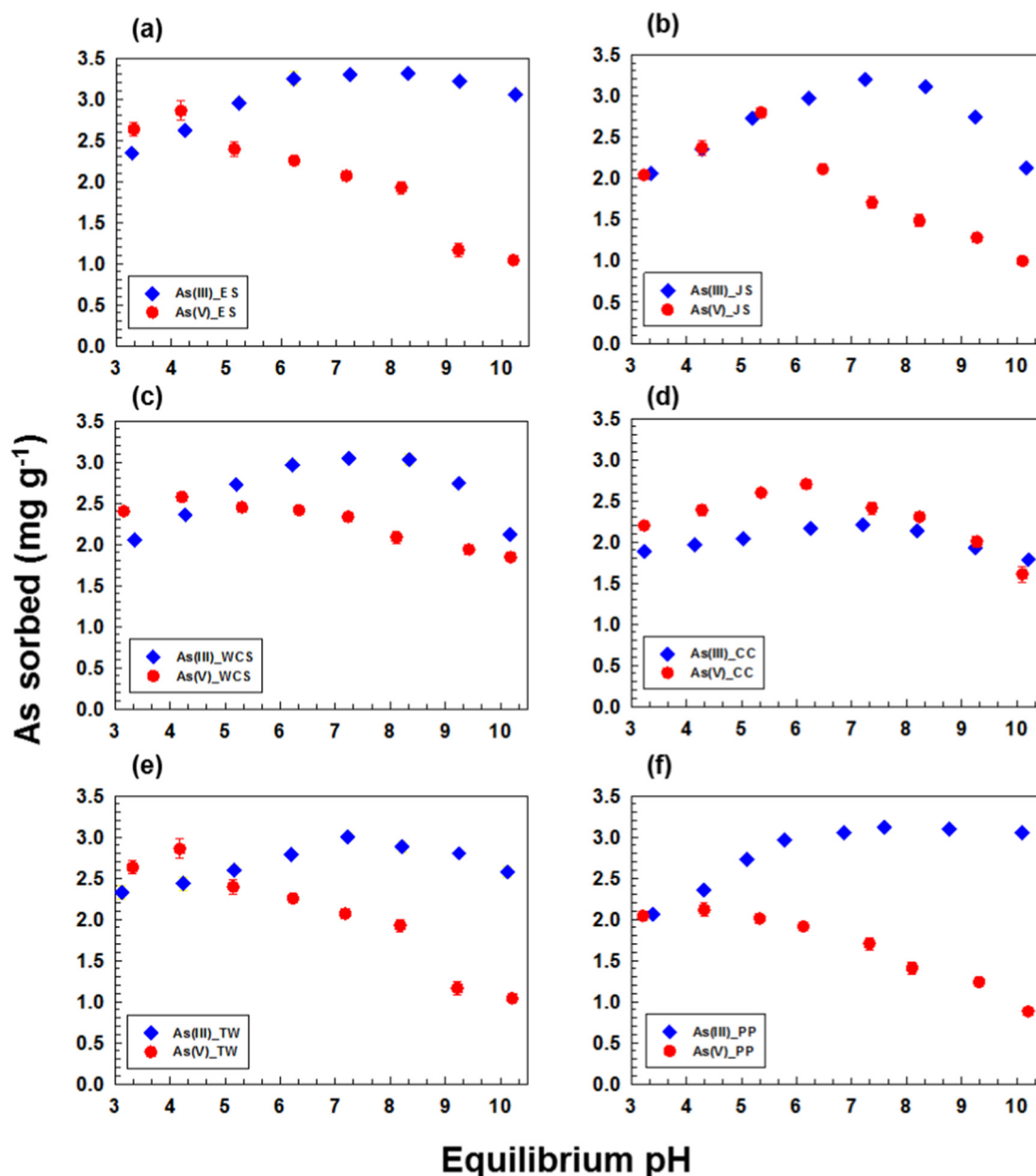
Fig. 1. Effect of pH on As(III) and As(V) biosorption (mg g^{-1}) by (a) egg shell (ES), (b) java plum seed (JS), (c) water chestnut shell (WCS), (d) corn cob (CC), (e) tea waste (TW) and (f) pomegranate peel (PP) at initial As(III) concentration of 4 mg L^{-1}, biosorbent dose of 1 g L^{-1} and at 20 °C. Values are shown as mean ± standard error (n = 3).

surface of biosorbents.

The maximum sorption of both species of As by egg shell and java plum seed could be attributed to transfer of As from solution to biosorbent surface (Ranjan et al., 2009). As the egg shell and java plum seed contained higher surface pores and available reactive sites (Table 1), more As(III) (at high pH) and As(V) (at low pH) were removed by egg shell and java plum seed than other biosorbents.

3.2. Isotherm modeling

Freundlich model showed that coefficient of variation (R^2) spanned 0.81–0.96 for As(III) and 0.87–0.95 for As(V) sorption (Figs. 3 and 4; Table 2). Sorption affinity, Q_F, values spanned 1.79–2.64 and 1.64–2.40 mg^{1-n} g^{-1} L^n for As(III) and As(V), respectively (Table 2). Water chestnut shell (2.64 and 2.4 mg^{1-n} g^{-1} L^n) and egg shell (1.98 and 2.0 mg^{1-n} g^{-1} L^n) achieved the greatest Q_F values for As(III) and As

(V) (Figs. 3 and 4; Table 2). Sorption intensity, n, ranged from 1.85 to 2.87 and 2.63–3.23, for As(III) and As(V), respectively (Table 2). The parameter n is considered as a measure of the extent in heterogeneity of biosorbent sorption sites, thus a higher n value exhibits a greater surface heterogeneity (Abid et al., 2016; Okafor et al., 2012). In the current study, egg shell and java plum seed showed the highest n values both for As(III) (2.87 and 2.86, respectively) and As(V) (3.23 and 3.15, respectively), indicating their relatively more heterogeneous structure compared to the other biosorbents (Table 2).

For Langmuir model, R^2 ranged from 0.95 to 0.99 for As(III) and 0.95–0.98 for As(V) (Figs. 3 and 4; Table 2). Relatively (2–3 times) greater Q_L was observed for As(III) and As(V) sorption on egg shell and water chestnut shell compared to other biosorbents (Table 2).

Langmuir model provided better fit to As(III) and As(V) sorption than the Freundlich model implying that monolayer sorption is a dominant process of removal by biosorbents (Lugo-Lugo et al., 2012).
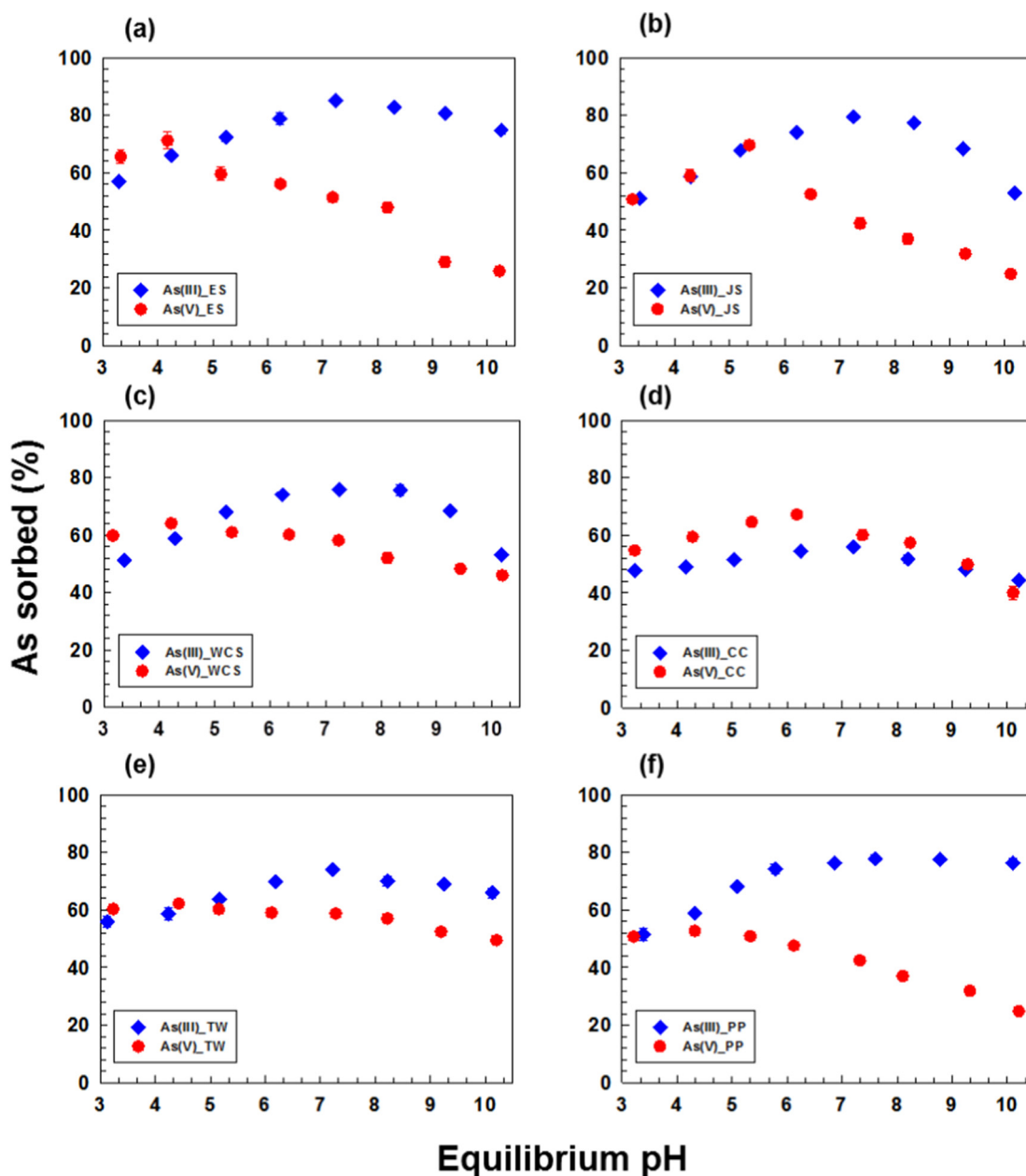
Fig. 2. Effect of pH on As(III) and As(V) percentage (%) removal by (a) egg shell (ES), (b) java plum seed (JS), (c) water chestnut shell (WCS), (d) corn cob (CC), (e) tea waste (TW) and (f) pomegranate peel (PP) at initial As(V) concentration of $4\,mg\,L^{-1}$, biosorbent dose of $1\,g\,L^{-1}$ and at 20 °C. Data are presented as mean ± standard error (n = 3).

Temkin model showed relatively higher R^2 for both As species sorption by egg shell and tea waste compared to other biosorbents (Figs. 3 and 4; Table 2). The low heat of sorption values (*b*) were obtained for both As species removal by egg shell and java plum seed derived biosorbents (Table 2), indicating linear decline in *b* established the greater coverage of both As species onto biosorbents (Foo and Hameed, 2010).

For the Dubinin–Radushkevich isotherm model, R^2 ranged from 0.95 to 0.99 for both As forms (Figs. 3 and 4; Table 2). Corn cob and tea waste showed higher R^2 for As(III) while pomegranate peel, water chestnut shell and java plum seed displayed higher R^2 for As(V), respectively than other biosorbents. The bonding energy (*E*) was also calculated for As(III) and As(V) sorption on biosorbents for Dubinin–Radushkevich model. If $E < 8\,kJ\,g^{-1}$ the physical sorption takes place and governed by pore filling process; if *E* spans $8–16\,kJ\,g^{-1}$, it describes the dominance of ion exchange and chemisorption

mechanisms (Memon et al., 2009; Abid et al., 2016). While, if *E* values are higher than $16\,kJ\,g^{-1}$, particle diffusion drives the sorption. In this study, *E* values ranged from 0.04 to $0.07\,kJ\,g^{-1}$ for both As species (Table 2), representing that physical sorption may be a dominant mechanism to bind As(III) and As(V) on the surface of biosorbents (Ahmad et al., 2013). However, extremely low *E* values may indicate that this model is not suitable to describe As(III/V) sorption onto biosorbents tested in the current study.

Our data showed that Langmuir model provided the highest R^2 values for As(III) and As(V) sorption to the biosorbents compared to other isotherm models. Separation factors (R_L) were computed for Langmuir model describing the favorability for As sorption (Fig. A.1; Supplementary material). The values of R_L are explained as: $R_L > 1$, $R_L = 1$, $0 < R_L < 1$, $R_L = 0$ then sorption process is unfavorable, linear, favorable, and irreversible, respectively (Mohan et al., 2011). In this study, R_L values ranged from 0.03–0.99 and 0.05–0.98 for As(III)
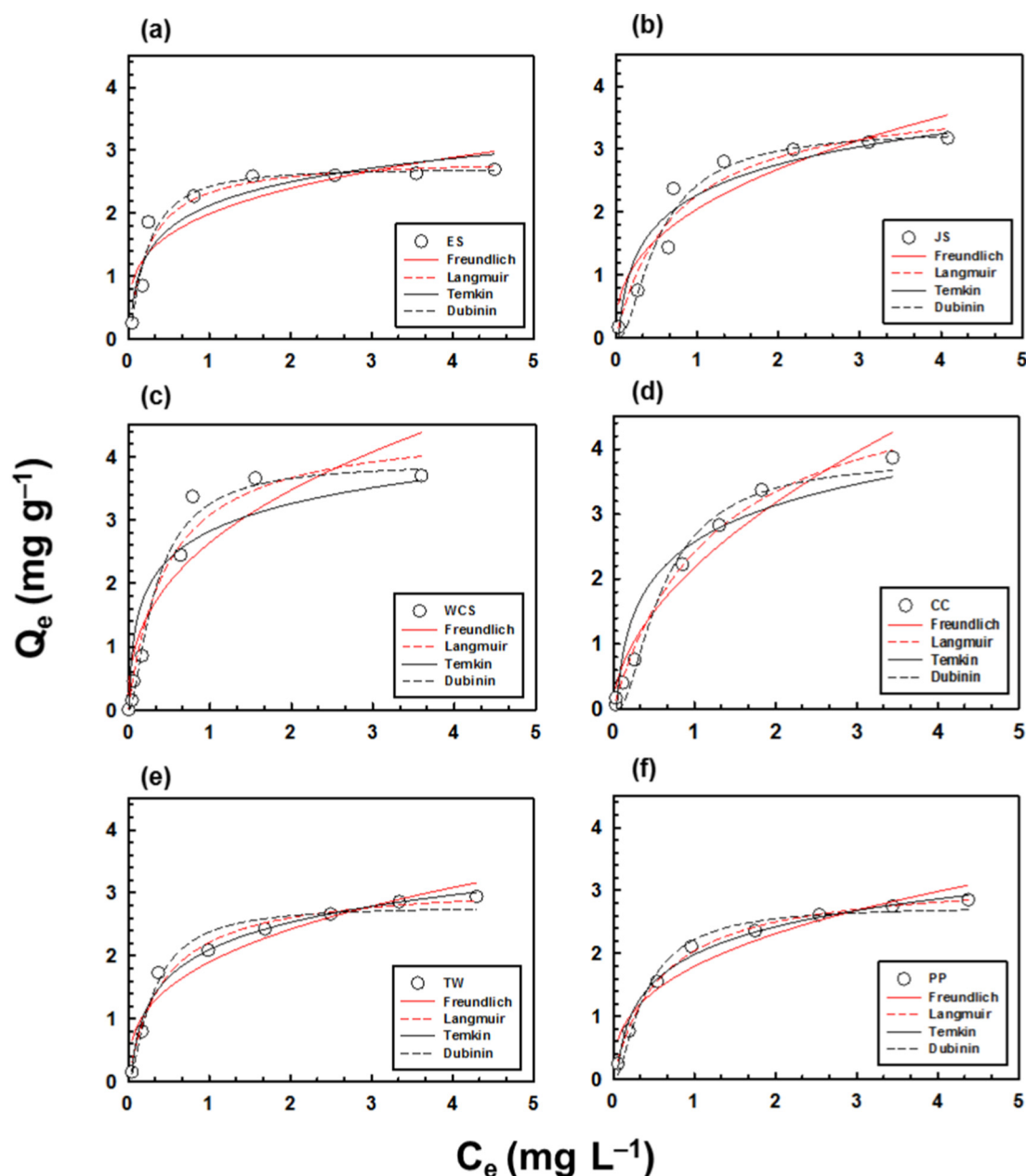
Fig. 3. Freundlich, Langmuir, Temkin and Dubinin-Radushkevich sorption isotherms of As(III) for (a) egg shell (ES), (b) java plum seed (JS), (c) water chestnut shell (WCS), (d) corn cob (CC), (e) tea waste (TW) and (f) pomegranate peel (PP) at biosorbent dose of 1 g L^{-1} and at 20 °C. The solid ($- - -$) line represents the model fits of the experimental data and black circles (●) indicate experimental data.

and As(V), respectively, which were < 1 for all the biosorbents. This indicates that sorption process was favorable, although As sorption was found to be the more favorable for egg shell and java plum seed than that of the other biosorbents.

3.3. Kinetic modeling

Kinetic models can explain the behavior of batch sorption system under varying experimental conditions and are useful for process optimization or scale up studies (Nadeem et al., 2015). Therefore, the pseudo-first and the pseudo-second order kinetic models were employed to determine rate of sorption for both species of As (Table 3; Fig. A.2, Supplementary material).

The R^2 for pseudo-second order model spanned 0.92–0.99 and 0.97–0.99 for As(III) and As(V), respectively, which are greater than the R^2 values (0.5–0.90 and 0.71–0.90, respectively) of pseudo-first order

model (Table 3). The q_e (cal) values of pseudo-first order model (1.69–3.49 mg g^{-1} for As(III) and 1.20–4.98 mg g^{-1} for As(V)) did not well fit the experimental data. However, the pseudo-second order provided the best fit for kinetic data, and q_e (cal) ranged from 2.64 to 3.26 mg g^{-1} for As(III) and 2.24–3.55 mg g^{-1} for As(V).

The pseudo-second order model with higher R^2 values and q_e values better explained the kinetics data, assuming that biosorption could be the rate limiting phase which may involve exchange of electrons or valence forces sharing between the biosorbent and sorbate (As) (Özacar and Sengil, 2003). Moreover, higher R^2 both for As(III) (0.99) and As(V) (0.99) onto egg shell and java plum seed calculated by pseudo-second-order also proved that sorption was more favorable by egg shell and java plum seed than the other biosorbents.
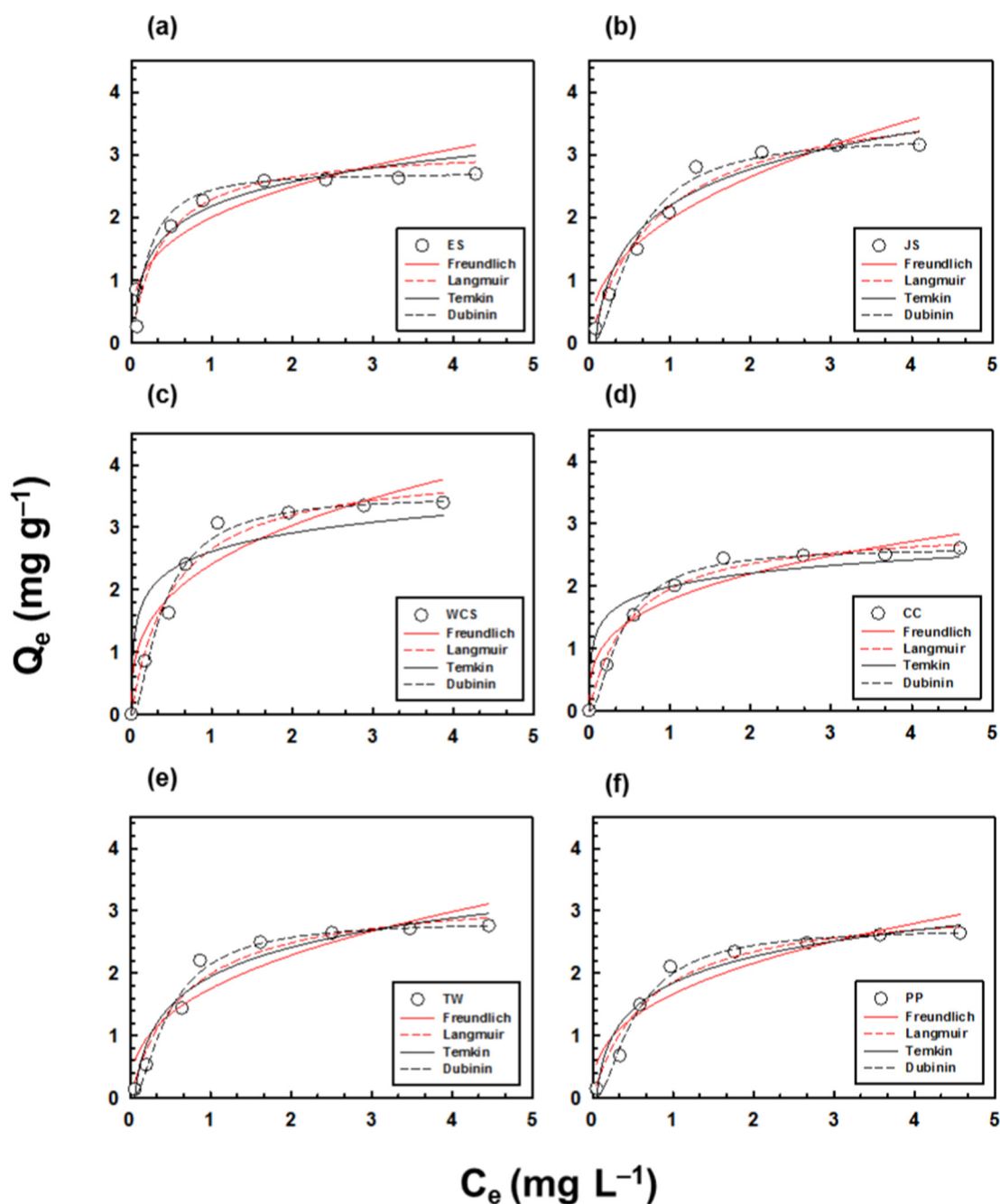
Fig. 4. Freundlich, Langmuir, Temkin and Dubinin-Radushkevich sorption isotherms of As(V) for (a) egg shell (ES), (b) java plum seed (JS), (c) water chestnut shell (WCS), (d) corn cob (CC), (e) tea waste (TW) and (f) pomegranate peel (PP) at biosorbent dose of 1 g L^{-1} and 20 °C. The solid ($-\,-\,-$) line represents the model fits of the experimental data and black circles (●) indicate experimental data.

3.4. Contact (equilibrium) time for As sorption

Figs. A.3, A.4 in the Supplementary material show results of contact time study for As(III) and As(V) removal by the different biosorbents in batch systems. Biosorbent dose was 1 g L^{-1} and 4 mg L^{-1} initial As(III) and As(V) concentration was used for all the experiments. The As(III) and As(V) removal by the biosorbents achieved equilibrium after 2 h of shaking, yielding maximum removal of 65–83% of As(III) and 63–80% of As(V) after which rise in contact time had negligible influence on As removal (Figs. A.3, A.4, Supplementary material). The highest sorption obtained at 2 h contact time could be due to the maximum affinity of biosorbents and reach at equilibrium, and after that a desorption could be started as it was slightly evident from kinetic data.

3.5. Biosorbent dose effect on As sorption

The impact of biosorbent dose (1–16 g L^{-1}) on the efficiency of sorption was also determined (Figs. A.5, A.6, Supplementary material). It was determined that As(III) and As(V) sorption decreased with maximum removal of both As(III) (3.4 mg g^{-1}) and As(V) (3.5 mg g^{-1}) obtained at the dose of 1 g L^{-1} (Figs. A.5, A.6, Supplementary material).

Egg shell and java plum seed showed more sorption capacity than the other biosorbents (Figs. A.5, A.6; Supplementary material).

Table 2
The parameters of different isotherm models for As(III) and As(V) biosorption onto various biosorbents at initial As concentration of 0.01–7 mg L⁻¹, 1 g L⁻¹ biosorbent dose and 20 °C temperature.

Arsenic species	Biosorbent	Langmuir[a]			Freundlich[a]			Temkin[a]			Dubininin-Radushkevich[a]		
		Q_L (mg g⁻¹)	K_L (L g⁻¹)	R^2	Q_F (mg^{1-n} g⁻¹ L^n)	n	R^2	b	A	R^2	Q_D (mg g⁻¹)	E (kJ g⁻¹)	R^2
As(III)	Egg shell	11.69 ± 2.5	4.03 ± 0.76	0.96**	1.98 ± 0.09	2.87 ± 0.34	0.81*	0.54 ± 0.04	50.58 ± 6.32	0.91**	2.70 ± 1.10	0.07 ± 0.003	0.95**
	Java plum seed	4.63 ± 0.65	1.13 ± 0.09	0.97**	2.05 ± 0.21	2.86 ± 0.32	0.87**	0.71 ± 0.01	25.44 ± 2.43	0.89**	3.29 ± 0.87	0.04 ± 0.001	0.96**
	Water chestnut shell	9.61 ± 1.21	2.12 ± 0.42	0.97**	2.64 ± 0.21	2.80 ± 0.65	0.86*	0.62 ± 0.01	90.47 ± 7.43	0.82*	3.88 ± 0.42	0.07 ± 0.001	0.96**
	Corn cob	4.33 ± 0.76	0.79 ± 0.03	0.95*	2.17 ± 0.34	1.85 ± 0.23	0.96**	0.81 ± 0.01	23.75 ± 2.20	0.90*	3.85 ± 1.02	0.04 ± 0.002	0.98**
	Tea waste	7.36 ± 1.28	2.32 ± 0.34	0.98**	1.89 ± 0.07	2.83 ± 0.76	0.92**	0.68 ± 0.02	28.08 ± 5.21	0.98**	2.78 ± 0.53	0.07 ± 0.003	0.97**
	Pomegranate peel	5.57 ± 1.32	1.73 ± 0.35	0.99**	1.79 ± 0.02	2.78 ± 0.55	0.94**	0.64 ± 0.05	22.41 ± 4.1	0.98**	2.74 ± 0.45	0.05 ± 0.009	0.97**
As(V)	Egg shell	8.43 ± 2.1	2.69 ± 0.32	0.96**	2.00 ± 0.21	3.23 ± 0.54	0.95**	0.55 ± 0.24	50.43 ± 5.21	0.95**	2.70 ± 0.65	0.07 ± 0.008	0.89**
	Java plum seed	4.62 ± 0.43	1.13 ± 0.12	0.97**	1.97 ± 0.32	3.15 ± 0.23	0.89**	0.85 ± 0.20	13.37 ± 2.32	0.95**	3.28 ± 0.92	0.04 ± 0.001	0.97**
	Water chestnut shell	7.73 ± 0.9	1.93 ± 0.4	0.98**	2.40 ± 0.67	3.02 ± 0.23	0.91**	0.42 ± 0.06	16.21 ± 2.12	0.82*	3.50 ± 1.11	0.05 ± 0.006	0.97**
	Corn cob	5.71 ± 0.32	1.92 ± 0.21	0.98**	1.77 ± 0.23	3.13 ± 0.43	0.93**	0.31 ± 0.05	6.11 ± 1.32	0.85*	2.61 ± 0.48	0.05 ± 0.002	0.96**
	Tea waste	4.92 ± 1.21	1.48 ± 0.37	0.96**	1.75 ± 0.02	2.63 ± 0.41	0.87**	0.67 ± 0.23	17.49 ± 2.21	0.94**	2.82 ± 0.34	0.05 ± 0.005	0.95**
	Pomegranate peel	4.50 ± 0.42	1.42 ± 0.25	0.96**	1.66 ± 0.09	2.70 ± 0.33	0.88**	0.60 ± 0.21	20.63 ± 2.34	0.93**	2.71 ± 0.21	0.04 ± 0.001	0.99**

* Significant correlation at $p < 0.05$.
** Significant correlation at $p < 0.01$.
[a] Mean ± SE values.

3.6. Initial As concentration effect on As sorption

Effect of the initial As(V) or As(III) (0.01–7 mg L⁻¹) concentration was studied at a biosorbent dose of 1 g L⁻¹ and appropriate aqueous pH (obtained from the pH experiments for each biosorbent) for As(III) and As(V) sorption (Figs. A.7, A.8; Supplementary material).

The results demonstrated that egg shell and java plum seed had the highest sorption capacity for As(III) (3.50 mg g⁻¹ and 3.31 mg g⁻¹, respectively) at the added concentration of 1 g L⁻¹ (Fig. A.7a, b; Supplementary material) and for As(V) it was 3.45 mg g⁻¹ and 3.27 mg g⁻¹, respectively at the added concentration 1 g L⁻¹ (Fig. A.8a, b; Supplementary material). With increasing the As concentration up to 4–5 mg L⁻¹, the sorption was found to increase for both As species. However further increase in As concentration showed no significant improvement in As sorption by all the biosorbents.

3.7. Surface characterization and As(III)/As(V) sorption possible mechanisms

3.7.1. FTIR spectroscopy

For surface functional group characterization (biochemical composition) and possible As(III) and As(V) sorption mechanism on the surface of biosorbents, FTIR spectra of As-loaded and -unloaded biosorbents were obtained in the wavenumber ranging from 400 to 4000 cm⁻¹ (Table A1; Supplementary material). The absorbance spectra of As-loaded and -unloaded egg shell and water chestnut shell are presented in Figs. 5, 6 and 7. For As-unloaded biosorbents, characteristics peaks at 3419, 3391, 3409, 3378, 3408 and 3399 cm⁻¹ of egg shell, water chest shell, corn cob, tea waste, java plum seed and PP, respectively, (Figs. 5a–d, 6a–d and 7a–d) could possibly indicate −OH stretching vibrations of macromolecular association, such as cellulose, lignin and pectin (Agrafioti et al., 2014).

The C−H stretching absorbance bands observed at 2875, 2924, 2920, 2920, 2928 and 2933 cm⁻¹ of egg shell, water chestnut shell, corn cob, tea waste, java plum seed and pomegranate peel, respectively (Figs. 5a, d, 6a, d and 7a, d) might be associated with alkyl surface functional groups (i.e., methylene, methyl and methoxy) of biosorbents (Nadeem et al., 2015).

The spectral bands located at 1799, 1622l, 1733, 1650, 1619 and 1726 cm⁻¹ for egg shell, water chestnut shell, corn cob, tea waste, java plum seed and pomegranate peel, respectively (Figs. 5a, d, 6a, d and 7a, d) could be attributed to C−O stretching vibrations of non-ionic carboxyl surface functional moieties (−C=O) including −COOH and −COOCH₃ which might be associated with carboxylic acids and the ester functional groups of the lipids (Feng et al., 2011; Lasheen et al., 2012).

The symmetric and asymmetric vibration peaks found at 1424, 1371, 1515, 1535, 1366 and 1506 cm⁻¹ of egg shell, water chestnut shell, corn cob, tea waste, java plum seed and pomegranate peel, respectively (Figs. 5a, d, 6a, d and 7a, d) could be from ionic carboxylic groups (COO⁻) of pectin, proteins or hemicellulose (Tuna et al., 2013; Nadeem et al., 2015). The peaks observed at 875, 862 and 877 of egg shell, java plum seed and pomegranate peel (Figs. 5a, d and 7a, d). respectively, might be due to the stretching vibrations of −NH₂ in proteins (Yang and Jiang, 2014; Abid et al., 2016).

The FTIR spectra of all the As(III)-loaded biosorbents showed both positive and negative changes in the wavenumbers (Figs. 1b, e, 2b, e and 3b, e). The −OH peaks of egg shell, water chestnut shell, corn cob, tea waste, java plum seed and pomegranate peel were shifted to 3409, 3355, 3405, 3380, 3373 and 3454 cm⁻¹, respectively (Figs. 5b, e, 6b, e and 7b, e). The −C−H stretching absorbance bands were shifted to 2878, 2933, 2918, 2921, 2927 and 2912 cm⁻¹ for egg shell, water chestnut shell, corn cob, tea waste, java plum seed and pomegranate peel, respectively (Figs. 5b, e, 6b, e and 7b, e). The C−O peaks of the non-ionic carboxyl surface functional groups (−C=O) were slightly changed to 1624, 1734, 1660, 1647 and 1726 cm⁻¹ for water chestnut

Table 3
Kinetic modeling equations parameters values for As biosorption onto various biosorbents at initial As concentration of 0.01–7 mg L^{-1}, 1 g L^{-1} biosorbent dose, and 20 °C temperature.

	Biosorbent	Pseudo-first-order model[a]			Pseudo-second-order model[a]		
		q_e (mg g^{-1})	k_1 (min^{-1})	R^2	q_e (mg g^{-1})	k_2 (g mg^{-1} min^{-1})	R^2
As(III)	Egg shell	2.65 ± 0.56	0.1 ± 0.03	0.84*	2.65 ± 0.2	0.37 ± 0.09	0.99*
	Java plum seed	3.24 ± 0.43	0.08 ± 0.01	0.98**	2.98 ± 0.11	0.33 ± 0.05	0.99*
	Water chestnut shell	2.01 ± 0.43	0.3 ± 0.65	0.80*	2.64 ± 0.11	0.29 ± 0.03	0.97*
	Corn cob	3.49 ± 0.14	0.12 ± 0.03	0.71*	2.98 ± 0.42	0.34 ± 0.02	0.98**
	Tea waste	1.69 ± 0.12	0.23 ± 0.34	0.90**	3.26 ± 0.90	0.31 ± 0.04	0.92**
	Pomegranate peel	2.01 ± 0.20	0.30 ± 0.12	0.82*	2.7 ± 1.1	0.37 ± 0.10	0.99**
As(V)	Egg shell	1.20 ± 0.18	0.03 ± 0.001	0.71*	2.82 ± 0.40	0.35 ± 0.06	0.99**
	Java plum seed	2.53 ± 0.18	0.40 ± 0.07	0.97**	2.77 ± 0.23	0.36 ± 0.04	0.99**
	Water chestnut shell	1.81 ± 0.12	0.3 ± 0.02	0.94*	3.55 ± 0.21	0.28 ± 0.07	0.95**
	Corn cob	4.98 ± 1.23	0.69 ± 0.12	0.64*	3.55 ± 0.42	0.28 ± 0.12	0.98**
	Tea waste	1.03 ± 0.23	0.01 ± 0.001	0.67*	2.72 ± 0.90	0.36 ± 0.02	0.96**
	Pomegranate peel	1.42 ± 0.13	0.015 ± 0.01	0.50*	2.24 ± 0.21	0.45 ± 0.02	0.97**

* Significant correlation at $p < 0.05$.
** Significant correlation at $p < 0.01$.
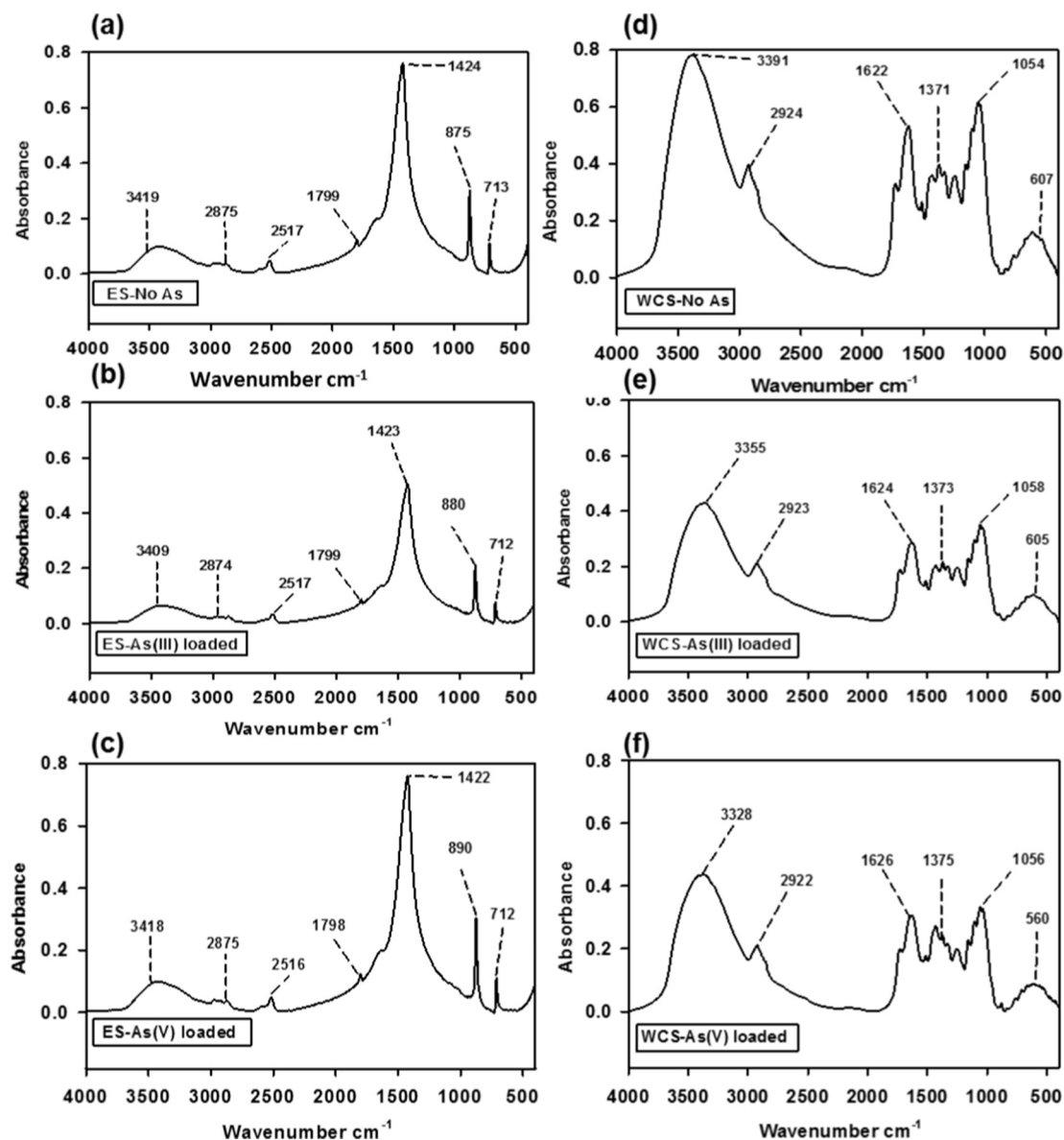[a] Mean ± SE values.

Fig. 5. The FTIR absorbance spectra of egg shell (ES) and water chestnut shell (WCS), (a, d) no As loading, (b, e) As(III)-loaded, and (c, f) As(V)-loaded.
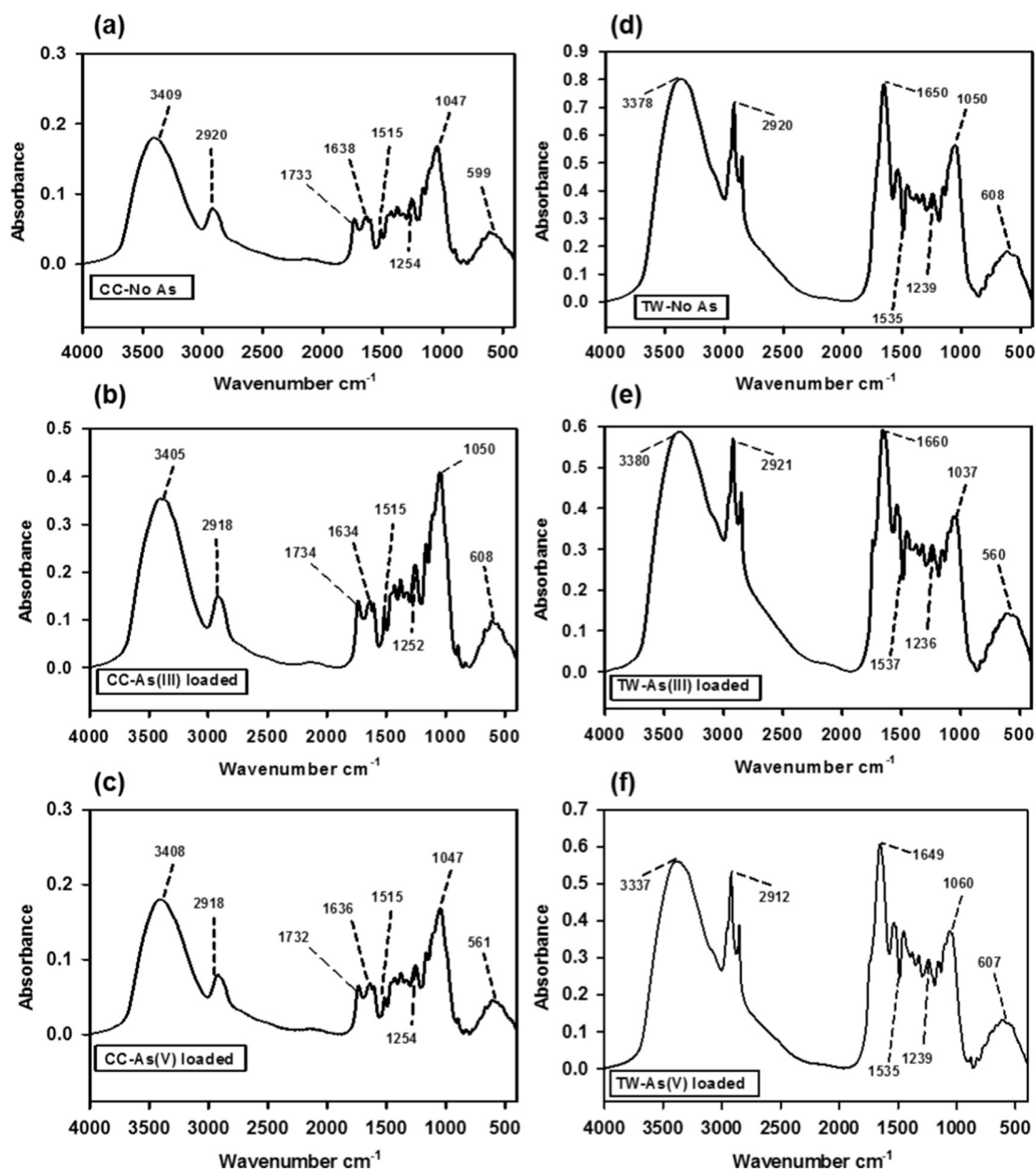
Fig. 6. The FTIR absorbance spectra of corn cob (CC) and tea waste (TW), (a, d) no As loading, (b, e) As(III) = loaded and (c, f) As(V)-loaded.

shell, corn cob, tea waste, java plum seed and pomegranate peel, respectively (Figs. 5b, e, 6b, e and 7b, e). The peaks possibly indicating the carboxylic groups (−COO⁻) egg shell, water chestnut shell, corn cob, tea waste, java plum seed and pomegranate peel were shifted to 1424, 1373, 1515, 1537, 1365 and 1563 cm⁻¹, respectively (Figs. 5b, e, 6b, e and 7b, e). Moreover, the possible spectral bands for −NH₂ group of egg shell, java plum seed and pomegranate peel were changed to 880, 860 and 832 cm⁻¹, respectively (Figs. 5b, 7b and e).

Similarly, the FTIR spectra of As(V)-loaded biosorbents were also recorded (Figs. 5c, f, 6c, f and 7c, f). The −OH spectral bands of As(V)-unloaded egg shell, water chestnut shell, corn cob, tea waste, java plum seed and pomegranate peel, were shifted to 3418, 3328, 3408, 3337, 3405 and 3353 cm⁻¹, respectively (Fig. 5c, f, 6c, f and 7c, f). The C−H stretching vibrations were changed to 2875, 2922, 2918, 2912, 2918, 2922 cm⁻¹ for egg shell, water chestnut shell, corn cob, tea waste, java plum seed and pomegranate peel, respectively. The shift in −C=O peaks was observed as 1798, 1626, 1732, 1649, 1634 and 1726 cm⁻¹ for egg shell, water chestnut shell, corn cob, tea waste, java plum seed

and pomegranate peel, respectively (Figs. 5c, f, 6c, f and 7c, f. The shift in −COO⁻ group of egg shell, water chestnut shell, corn cob, tea waste, java plum seed and pomegranate peel was observed to the wavenumbers of 1422, 1375, 1515, 1535, 1376 and 1513 cm⁻¹, respectively (Figs. 5c, f, 6c, f and 7c, f). The peaks for –NH₂ groups of egg shell, java plum seed and pomegranate peel were shifted to 890, 897 and 877 cm⁻¹, respectively (Figs. 5c, f, 6c, f and 7c, f).

These shifts in spectral peaks might be ascribed to the As(III) and As (V) ions association with the functional groups (−OH, alkyl, −COO⁻) of biosorbents via surface complexation and/or ion exchange (Wu et al., 2017). Moreover, according to previous studies, these shifts in the spectral peaks were possibly due to As−O vibrations which showed that oxygen-rich functional groups were mainly responsible for the successful sorption of both As species (Hu et al., 2015; Zhou et al., 2017; Borah et al., 2009).

A slight shift in characteristic peaks of −NH₂ in egg shell, java plum seed and pomegranate peel spectra indicates As(III) and As(V) association and/or complexation with −NH₂ moieties from protein
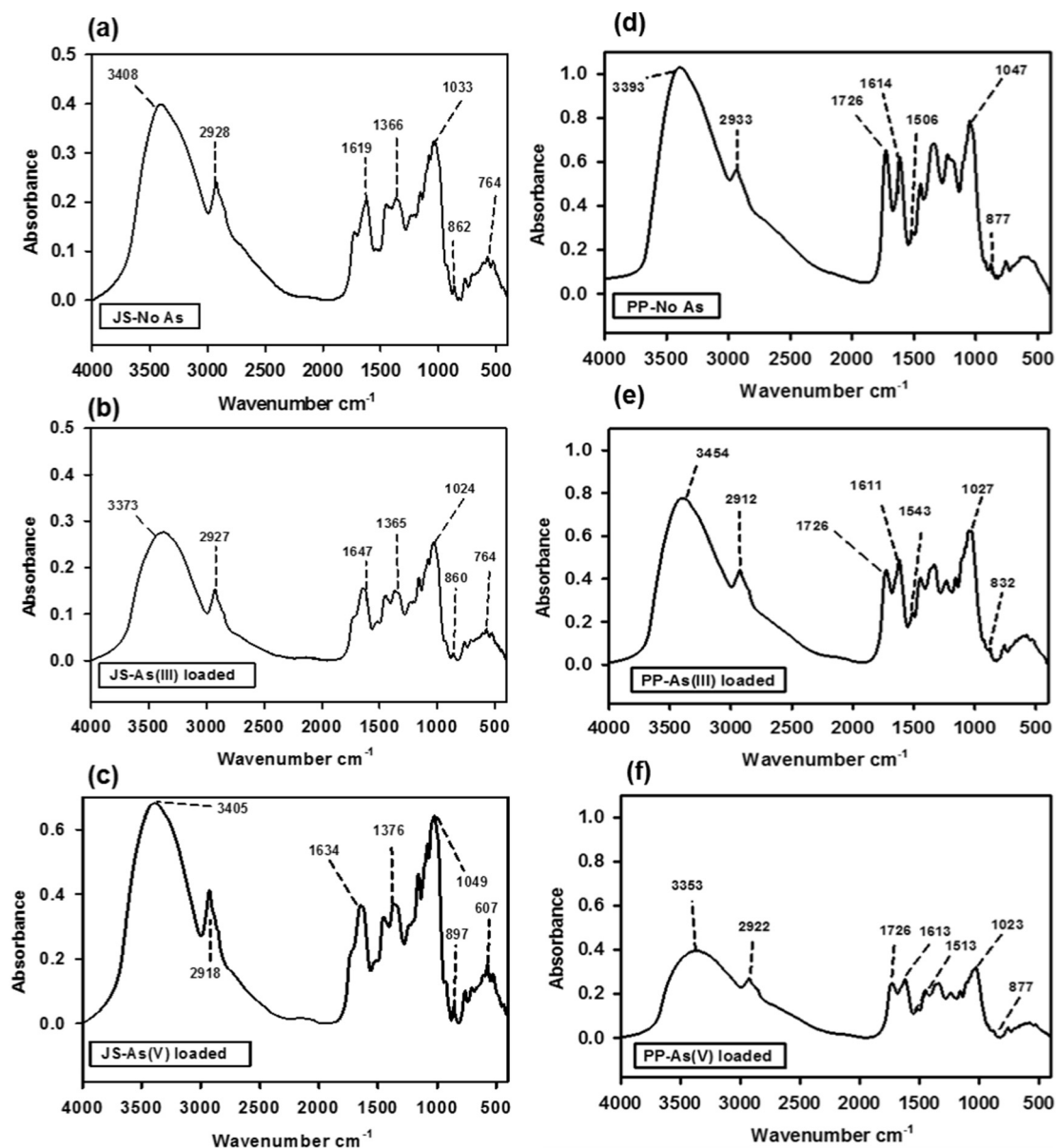
Fig. 7. The FTIR absorbance spectra of java plum seed (JS) and pomegranate peel (PP), (a, d) no As loading, (b, e) As(III)-loaded and (c, f) As(V)-loaded.

molecules of these biosorbents. Our data revealed that mainly −OH, alkyl and −COO⁻ functional groups (as indicated by negative or positive shifts in the peaks) could be involved in As(III) and As(V) sorption on the biosorbents. Notably, −NH₂ group was also responsible for As(III) and As(V) sorption by egg shell, java plum seed and pomegranate peel (Kumari et al., 2006; Haldhar et al., 2007; Zhang et al., 2018).

3.7.2. SEM-EDX analysis

Surface micro- and meso-morphology of the egg shell (selected due to the highest As removal) was examined pre- and post-As(III)/As(V) sorption by using the SEM (Fig. A.9, Supplementary material). The SEM analyses showed that As-unloaded biosorbent showed the abundance of porous (rough, heterogeneous and thread-like structures) (Fig. A.9a, Supplementary material). After loading of As(III)/As(V) species, the egg shell surface appeared to be relatively smooth possibly due to filling of porous structure with As anions (see Fig. A.9b, c, Supplementary material). The abundance of micro-cavities on the egg shell could play a key role in sequestering and removing As from water which was also evident from the largest SSA of the biosorbent in this study (Table 1) (Kamsonlian et al., 2012; Ebrahimi et al., 2014).

To estimate the elemental composition of egg shell, SEM-EDX analysis was carried out (Figs. A.9, A10 in Supplementary material). The SEM-EDX data did not detect the presence of As(III) or As(s) onto biosorbent, which indicates that EDX was unable to quantify the low As concentrations on biosorbent in this study. Future research is warranted to employ some advanced techniques such as Nano-SIMS to examine As distribution on biosorbents surface.

3.8. Desorption experiments

Desorption of sorbed As(III) and As(V) from As-loaded biosorbents was carried out in order to evaluate their regeneration ability which is considered important in practical application of water treatment process (Fig. A.10; Supplementary material). For this purpose, desorption was done by using 0.1 M NaOH upto four sorption/desorption cycles (Fig. A.11; Supplementary material). In the first sorption/desorption cycle, 68–97% of As(III) was removed from the biosorbents with the maximum desorption yielded by egg shell (97%) > waterchest nut shell (76%) > java plum seed (74%) (Fig. A.11a; Supplementary material). However, in the second, third and fourth cycles, As(III)

desorption efficiency was decreased up to 20–40% by all the biosorbents.

Similarly, 51–96% As(V) was desorbed in the first cycle which was reduced to 43–84% in the fourth desorption cycle (Fig. A.11b; Supplementary material). Egg shell (94%) and java plum seed (86%) showed the greatest desorption potential for As(V). The decrease in desorption ability with increasing desorption cycles might be attributed to strong effect of NaOH exerted on the molecules of biological tissues and desorbing maximum concentration of As from the surface of biosorbents, thereby its use as desorbing agent is only beneficial for 1 desorption cycle (Rahaman et al., 2008). Our results revealed that egg shell and java plum seed have the highest desorption capability for both species of As.

3.9. Environmental significance and implications

The results demonstrated that the studied biosorbents, in particular the egg shell and java plum seed, showed more As(III) and As(V) sorption than other biosorbents and immobilized 85–87% of As(III) and 67–71% of As(V). It reveals that 1 g of powdered egg shell and/or java plum seed is enough to remove As less than the WHO permissible limit ($10 \, \mu g \, L^{-1}$) in 1 L of As-contaminated drinking water.

The used biowaste could be transformed into ash by burning at relatively less temperature ($< 100 \, ^{\circ}C$) in order to reduce volatilization of As and safe disposal of the As-loaded biosorbents at a proper landfill site (Sas-Nowosielska et al., 2004).

In Table A2 of the Supplementary material, we compared the sorption capacity of biosorbents evaluated in our study with the previous studies. In this study, egg shell (3.38 and 2.69 mg g^{-1}) and java plum seed (3.22 and 2.80 mg g^{-1}) exhibited higher sorption both for As(III) and As(V), respectively, compared to some of the biosorbents used previously (Table A2; Supplementary material). Hence both egg shell and java plum seed have the highest As(III/V) sorption, and as such could serve as potential biosorbents for As(III) and As(V) removal from drinking water.

The production cost of biosorbents may vary and reach up to U\$386 ton^{-1} (Norgate and Langberg, 2009), therefore, using biosorbents might be a more economical option compared to activated carbon (U\$1500 ton^{-1}) (Moreira et al., 2017) and zeolite (U\$600 ton^{-1}) (Hina et al., 2015). Cost-benefit analysis of our study revealed that 20 L of drinking water can be treated with 20 g of biosorbent in a low-cost household type filter. This may indicate that the As filtration technology developed from these biosorbents would be very much economical and sustainable, especially for the developing countries like Pakistan.

4. Conclusions

This study shows that the egg shell and java plum seed have a great potential for effective remediation of As-contaminated water and removed 87% and 78% of As(III) and 71% and 67% of As(V), respectively. The highest As(III) removal was obtained at pH 7 both for egg shell and java plum seed, while the maximum removal of As(V) was observed at pH 4 and 5.3 for egg shell and java plum seed, respectively. This indicates that, in the case of As(V) removal, egg shell proved to be more effective at acidic pH than the java plum seed. Langmuir isotherm model and pseudo-second order kinetic model were the best to fit experimental equilibrium data for sorption of As(III) and As(V) onto the biosorbents.

The FTIR analysis suggested that $-OH$, alkyl, $-COO^-$ and $-NH_2$ functional groups were involved in biosorption of As(III) and As(V). Moreover, desorption (recyclability and reuse) studies indicated that NaOH solution of 0.1 M could efficiently be employed as desorbing chemical with the maximum As(III/V) desorption (up to 97%) in the first cycle. While in subsequent cycles desorption potential reduced steadily up to 20–43% both for As(III) and As(V). This study unveils

that the egg shell and java plum seed could be employed as the effective, cheap and easily available biosorbents for the removal of As(III) and As(V) from As-contaminated drinking water.

Appendix A. Supplementary data

Supplementary data to this article can be found online at https://doi.org/10.1016/j.envint.2018.12.049.

References

Abid, M., Niazi, N.K., Bibi, I., Farooqi, A., Ok, Y.S., Kunhikrishnan, A., et al., 2016. Arsenic (V) biosorption by charred orange peel in aqueous environments. Int. J. Phytoremediation 18, 442–449.

Agrafioti, E., Kalderis, D., Diamadopoulos, E., 2014. Ca and Fe modified biochars as adsorbents of arsenic and chromium in aqueous solutions. J. Environ. Manag. 146, 444–450.

Ahmad, M., Lee, S.S., Rajapaksha, A.U., Vithanage, M., Zhang, M., Cho, J.S., et al., 2013. Trichloroethylene adsorption by pine needle biochars produced at various pyrolysis temperatures. Bioresour. Technol. 143, 615–622.

Aryal, M., Ziagova, M., Liakopoulou-Kyriakides, M., 2010. Study on arsenic biosorption using Fe (III)-treated biomass of Staphylococcus xylosus. Chem. Eng. J. 162, 178–185.

Ashraf, A., Bibi, I., Niazi, N.K., Ok, Y.S., Murtaza, G., Shahid, M., et al., 2017. Chromium (VI) sorption efficiency of acid-activated banana peel over organo-montmorillonite in aqueous solutions. Int. J. Phytoremediation 19, 605–613.

Bibi, S., Farooqi, A., Yasmeen, A., Kamran, M.A., Niazi, N.K., 2017. Arsenic and fluoride removal by potato peel and rice husk (PPRH) ash in aqueous environments. Int. J. Phytoremediation 19, 1029–1036.

Borah, D., Satokawa, S., Kato, S., Kojima, T., 2009. Sorption of As (V) from aqueous solution using acid modified carbon black. J. Hazard. Mater. 162, 1269–1277.

Dadwal, A., Mishra, V., 2016. Review on biosorption of arsenic from contaminated water. Clean: Soil, Air, Water. https://doi.org/10.1002/clen.201600364.

Ebrahimi, R., Maleki, A., Shahmoradi, B., Daraei, H., Mahvi, A.H., Barati, A.H., et al., 2014. Elimination of arsenic contamination from water using chemically modified wheat straw. Desalin. Water Treat. 51, 2306–2316.

Faruque, M.O., Uddin, M.J., 2012. Removal of arsenic from groundwater using burnt rice straw. Asian Trans. Eng. 2, 103–129.

Feng, N., Guo, X., Liang, S., Zhu, Y., Liu, J., 2011. Biosorption of heavy metals from aqueous solutions by chemically modified orange peel. J. Hazard. Mater. 185, 49–54.

Foo, K., Hameed, B., 2010. Insights into the modeling of adsorption isotherm systems. Chem. Eng. J. 156, 2–10.

Ghimire, K.N., Inoue, K., Yamaguchi, H., Makino, K., Miyajima, T., 2003. Adsorptive separation of arsenate and arsenite anions from aqueous medium by using orange waste. Water Res. 37, 4945–4953.

Haldhar, D., Sahoo, S., Mishra, P., 2007. Adsorption of As (III) from aqueous solution by groundnut shell. Swiss J. Appl. Sci. 2, 1–12.

Hering, J.G., Katsoyiannis, I.A., Theoduloz, G.A., Berg, M., Hug, S.J., 2017. Arsenic removal from drinking water: experiences with technologies and constraints in practice. Am. Soc. Civil Eng. https://doi.org/10.1061/(ASCE)EE.1943-7870.0001225.

Hina, K., Hedley, M., Camps-Arbestain, M., Hanly, J., 2015. Comparison of pine bark, biochar and zeolite as sorbents for NH4 + -N removal from water. Clean: Soil, Air, Water 43, 86–91.

Hsu, L.-I., Cheng, Y.-W., Chen, C.-J., Wu, M.-M., Hsu, K.-H., Chiou, H.-Y., et al., 2016. Cumulative arsenic exposure is associated with fungal infections: two cohort studies based on southwestern and northeastern basins in Taiwan. Environ. Int. 96, 173–179.

Hu, X., Ding, Z., Zimmerman, A.R., Wang, S., Gao, B., 2015. Batch and column sorption of

arsenic onto iron-impregnated biochar synthesized through hydrolysis. Water Res. 68, 206–216.

Igalavithana, A.D., Lee, S.-E., Lee, Y.H., Tsang, D.C., Rinklebe, J., Kwon, E.E., et al., 2017. Heavy metal immobilization and microbial community abundance by vegetable waste and pine cone biochar of agricultural soils. Chemosphere 174, 593–603.

Kaartinen, T., Laine-Ylijoki, J., Ahoranta, S., Korhonen, T., Neitola, R., 2017. Arsenic removal from mine waters with sorption techniques. Mine Water Environ. 36, 199–208.

Kamsonlian, S., Suresh, S., Ramanaiah, V., Majumder, C., Chand, S., Kumar, A., 2012. Biosorptive behaviour of mango leaf powder and rice husk for arsenic (III) from aqueous solutions. Int. J. Environ. Sci. Technol. 9, 565–578.

Khalid, S., Shahid, M., Niazi, N.K., Rafiq, M., Bakhat, H.F., Imran, M., et al., 2017. Arsenic behaviour in soil-plant system: biogeochemical reactions and chemical speciation influences. In: Enhancing Cleanup of Environmental Pollutants. Springer.

Kumari, P., Sharma, P., Srivastava, S., Srivastava, M.M., 2006. Biosorption studies on shelled *Moringa oleifera* Lamarck seed powder: removal and recovery of arsenic from aqueous system. Int. J. Miner. Process. 78, 131–139.

Lasheen, M.R., Ammar, N.S., Ibrahim, H.S., 2012. Adsorption/desorption of Cd (II), Cu (II) and Pb (II) using chemically modified orange peel: equilibrium and kinetic studies. Solid State Sci. 14, 202–210.

Lugo-Lugo, V., Barrera-DÃaz, C., Ureña-Núñez, F., Bilyeu, B., Linares-HernÃindez, I., 2012. Biosorption of Cr (III) and Fe (III) in single and binary systems onto pretreated orange peel. J. Environ. Manag. 112, 120–127.

Marín-Rangel, V.M., Cortés-Martínez, R., Cuevas Villanueva, R.A., Garnica-Romo, M.G., Martínez-Flores, H.E., 2012. As (V) Biosorption in an aqueous solution using chemically treated lemon (*Citrus aurantifolia* Swingle) residues. J. Food Sci. 77, 10–14.

Meharg, A.A., Rahman, M.M., 2003. Arsenic contamination of Bangladesh paddy field soils: implications for rice contribution to arsenic consumption. Environ. Sci. Technol. 37, 229–234.

Mehmood, T., Bibi, I., Shahid, M., Niazi, N.K., Murtaza, B., Wang, H., et al., 2017. Effect of compost addition on arsenic uptake, morphological and physiological attributes of maize plants grown in contrasting soils. J. Geochem. Explor. 178, 83–91.

Memon, S.Q., Bhanger, M., Khuhawar, M., 2009. Use of modified sorbent for the separation and preconcentration of chromium species from industrial waste water. J. Hazard. Mater. 163, 511–516.

Mohan, D., Rajput, S., Singh, V.K., Steele, P.H., Pittman, C.U., 2011. Modeling and evaluation of chromium remediation from water using low cost bio-char, a green adsorbent. J. Hazard. Mater. 188, 319–333.

Mondal, M.K., Garg, R., 2017. A comprehensive review on removal of arsenic using activated carbon prepared from easily available waste materials. Environ. Sci. Pollut. Res. 1–12.

Moreira, M., Noya, I., Feijoo, G., 2017. The prospective use of biochar as adsorption matrix—a review from a lifecycle perspective. Bioresour. Technol. 246, 135–141.

Nadeem, R., Manzoor, Q., Iqbal, M., Nisar, J., 2015. Biosorption of Pb (II) onto immobilized and native *Mangifera indica* waste biomass. J. Ind. Eng. Chem. 35, 185–195.

Naidu, R., Smith, E., Owens, G., Bhattacharya, P., Nadebum, P., 2006. Dynamics of Arsenic in Groundwater Samples. Managing Arsenic in the Environment: From Soil to Human Health. CSIRO Publishing, Victoria.

Narayanan, A.L., Dhamodaran, M., 2014. Removal of arsenic from aqueous solutions by lawsonia inerims carbon. Int. J. Pharm. Chem. Biol. Sci. 4, 19–35.

Niazi, N.K., Burton, E.D., 2016. Arsenic sorption to nanoparticulate mackinawite (FeS): an examination of phosphate competition. Environ. Pollut. 218, 111–117.

Niazi, N.K., Singh, B., Shah, P., 2011. Arsenic speciation and phytoavailability in contaminated soils using a sequential extraction procedure and XANES spectroscopy. Environ. Sci. Technol. 45, 7135–7142.

Niazi, N.K., Singh, B., Van Zwieten, L., Kachenko, A.G., 2012. Phytoremediation of an arsenic-contaminated site using *Pteris vittata* L. and *Pityrogramma calomelanos* var. austroamericana: a long-term study. Environ. Sci. Pollut. Res. 19, 3506–3515.

Niazi, N.K., Singh, B., Minasny, B., 2015. Mid-infrared spectroscopy and partial least-squares regression to estimate soil arsenic at a highly variable arsenic-contaminated site. Int. J. Environ. Sci. Technol. 12, 1965–1974.

Niazi, N.K., Bibi, I., Fatimah, A., Shahid, M., Javed, M.T., Wang, H., et al., 2017. Phosphate-assisted phytoremediation of arsenic by *Brassica napus* and *Brassica juncea*: morphological and physiological response. Int. J. Phytoremediation 19, 670–678.

Niazi, N.K., Bibi, I., Shahid, M., Ok, Y.S., Burton, E.D., Wang, H., et al., 2018a. Arsenic removal by perilla leaf biochar in aqueous solutions and groundwater: an integrated spectroscopic and microscopic examination. Environ. Pollut. 232, 31–41.

Niazi, N.K., Bibi, I., Shahid, M., Ok, Y.S., Shaheen, S.M., Rinklebe, J., et al., 2018b. Arsenic removal by Japanese oak wood biochar in aqueous solutions and well water: investigating arsenic fate using integrated spectroscopic and microscopic techniques. Sci. Total Environ. 621, 1642–1651.

Norgate, T., Langberg, D., 2009. Environmental and economic aspects of charcoal use in steelmaking. ISIJ Int. 49, 587–595.

Okafor, P.C., Okon, P.U., Daniel, E.F., Ebenso, E.E., 2012. Adsorption capacity of coconut (*Cocos nucifera* L.) Shell for Lead, copper, cadmium and arsenic from aqueous solutions. Int. J. Electrochem. Sci. 7, 12354–12369.

Özacar, Mahmut, Sengil, Ayhan, 2003. Adsorption of reactive dyes on calcined alunite from aqueous solutions. J. Hazard. Mater. 98, 211–224.

Prasad, K.S., Ramanathan, A., Paul, J., Subramanian, V., Prasad, R., 2014. Biosorption of arsenite (As^{+3}) and arsenate (As^{+5}) from aqueous solution by *Arthrobacter* sp. biomass. Environ. Technol. 34, 2701–2708.

Rahaman, M., Basu, A., Islam, M., 2008. The removal of As (III) and As (V) from aqueous solutions by waste materials. Biomagn. Res. Technol. 99, 2815–2823.

Ranjan, D., Talat, M., Hasan, S., 2009. Biosorption of arsenic from aqueous solution using agricultural residue rice polish. J. Hazard. Mater. 166, 1050–1059.

Rasheed, H., Slack, R., Kay, P., 2016. Human health risk assessment for arsenic: a critical review. Crit. Rev. Environ. Sci. Technol. 46, 1529–1583.

Sari, A., Tuzen, M., 2009. Biosorption of As (III) and As (V) from aqueous solution by macrofungus (*Inonotus hispidus*) biomass: equilibrium and kinetic studies. J. Hazard. Mater. 164, 1372–1378.

Sas-Nowosielska, A., Kucharski, R., Malkowski, E., Pogrzeba, M., Kuperberg, J.M., Krynski, A., 2004. Phytoextraction crop disposal - an unsolved problem. Environ. Pollut. 128, 373–379.

Shaheen, S.M., Eissa, F.I., Ghanem, K.M., El-Din, H.M.G., Anany, F.S.A., 2015. Metal ion removal from wastewaters by sorption on activated carbon, cement kiln dust, and sawdust. Water Environ. Res. 87, 506–515.

Shahid, M., Khalid, M., Dumat, C., Khalid, S., Niazi, N.K., Imran, M., et al., 2017. Arsenic level and risk assessment of groundwater in Vehari, Punjab Province, Pakistan. Exp. Health 1–11.

Shakoor, M.B., Niazi, N.K., Bibi, I., Rahman, M.M., Naidu, R., Dong, Z., et al., 2015. Unraveling health risk and speciation of arsenic from groundwater in rural areas of Punjab, Pakistan. Int. J. Environ. Res. Public Health 12, 12371–12390.

Shakoor, M.B., Niazi, N.K., Bibi, I., Murtaza, G., Kunhikrishnan, A., Seshadri, B., et al., 2016. Remediation of arsenic-contaminated water using agricultural wastes as biosorbents. Crit. Rev. Environ. Sci. Technol. 467–499.

Shakoor, M.B., Nawaz, R., Hussain, F., Raza, M., Ali, S., Rizwan, M., et al., 2017. Human health implications, risk assessment and remediation of As-contaminated water: a critical review. Sci. Total Environ. 601, 756–769.

Shakoor, M.B., Niazi, N.K., Bibi, I., Shahid, M., Sharif, F., Bashir, S., Shaheen, S.M., Wang, H., Tsang, D.C.W., Ok, Y.S., Rinklebe, J., 2018. Arsenic removal by natural and chemically modified water melon rind in aqueous solutions and groundwater. Sci. Total Environ. 645, 1444–1455.

Singh, R., Singh, S., Parihar, P., Singh, V.P., Prasad, S.M., 2015. Arsenic contamination, consequences and remediation techniques: a review. Ecotoxicol. Environ. Saf. 112, 247–270.

Smedley, P., Kinniburgh, D., 2002. A review of the source, behaviour and distribution of arsenic in natural waters. Appl. Geochem. 17, 517–568.

Tajernia, H., Ebadi, T., Nasernejad, B., Ghafori, M., 2014. Arsenic removal from water by sugarcane bagasse: an application of response surface methodology (RSM). Water Air Soil Pollut. 225, 1–22.

Tuna, A.Ö.A., Özdemir, E., Şimşek, E.B., Beker, U., 2013. Removal of As (V) from aqueous solution by activated carbon-based hybrid adsorbents: impact of experimental conditions. Chem. Eng. J. 223, 116–128.

Walton, K.S., Snurr, R.Q., 2007. Applicability of the BET method for determining surface areas of microporous metal-organic frameworks. J. Am. Chem. Soc. 129, 8552–8556.

Waqas, H., Shan, A., Khan, Y.G., Nawaz, R., Rizwan, M., Rehman, S.-U., et al., 2017. Human health risk assessment of arsenic in groundwater aquifers of Lahore, Pakistan. Hum. Ecol. Risk Assess. Int. J. 836–850.

Wu, C., Huang, L., Xue, S.-G., Huang, Y.-Y., Hartley, W., Cui, M.-q., et al., 2017. Arsenic sorption by red mud-modified biochar produced from rice straw. Environ. Sci. Pollut. Res. 24, 18168–18178.

Yang, G.-X., Jiang, H., 2014. Amino modification of biochar for enhanced adsorption of copper ions from synthetic wastewater. Water Res. 48, 396–405.

Zhang, X., Zhong, T., Chen, D., Cheng, M., Liu, L., Zhang, X., et al., 2016. Assessment of arsenic (As) occurrence in arable soil and its related health risk in China. Environ. Geochem. Health 38, 691–702.

Zhang, W., Liu, C., Zheng, T., Ma, J., Zhang, G., Ren, G., et al., 2018. Efficient oxidation and sorption of arsenite using a novel titanium (IV)-manganese (IV) binary oxide sorbent. J. Hazard. Mater. 353, 410–420.

Zhou, Z., Liu, Y.-G., Liu, S.-B., Liu, H.-Y., Zeng, G.-M., Tan, X.-F., et al., 2017. Sorption performance and mechanisms of arsenic (V) removal by magnetic gelatin-modified biochar. Chem. Eng. J. 314, 223–231.